The Canadian Mineralogist
Vol. 35, pp. 1465-1483 (1997)

ORE MINERALS OF THE COFER VOLCANOGENIC MASSIVE SULFIDE DEPOSIT, LOUISA COUNTY, VIRGINIA

J. WILLIAM MILLER[1]

Environmental Studies, University of North Carolina at Asheville, Asheville, North Carolina 28804, U.S.A.

JAMES R. CRAIG

Department of Geological Sciences, Virginia Polytechnic Institute and State University, Blacksburg, Virginia 24061, U.S.A.

ABSTRACT

The Cofer stratiform volcanogenic massive sulfide deposit is located near Mineral, Louisa County, Virginia. It consists of four major *en échelon* lenses that are essentially stratabound, with characteristics of both Cu–Zn and Zn–Pb–Cu types of volcanogenic massive sulfide deposits. Ore minerals include coarsely recrystallized pyrite with sphalerite and minor chalcopyrite, galena, arsenopyrite, and tetrahedrite-series minerals. Trace minerals include bornite, marcasite, pyrrhotite, mackinawite, molybdenite, covellite, digenite, chalcocite, gudmundite, boulangerite–bursaite, kobellite–tintinaite, meneghinite, cosalite, magnetite, ilmenite, rutile, native bismuth, and electrum. Major and minor ore minerals and most oxides were syngenetic with the host lower Cambrian Chopawamsic Formation and were subsequently recrystallized during metamorphism up to the lower amphibolite facies. Changes in the ore fluid after initial deposition resulted in a crude Zn/Pb *versus* Cu zoning and probably caused tetrahedrite–freibergite to be replaced by an arsenic- and iron-rich graphic intergrowth. Further re-equilibration during metamorphism resulted in exsolution of many sulfosalts, including tetrahedrite–freibergite associated with galena. The peak of metamorphism appears to have been at approximately 470°C, with sulfur activity in the range of –4.5 to –6.3 atmospheres.

Keywords: volcanogenic massive sulfide deposit, sulfosalts, tetrahedrite, tennantite, Cofer deposit, Gold–Pyrite Belt, Mineral District, Virginia.

SOMMAIRE

Le gisement stratiforme de Cofer, un amas de sulfures massifs volcanogéniques, est situé près de Mineral, dans le comté de Louisa, en Virginie. Il est fait de quatre lentilles majeures disposées *en échelon*, conformes au litage sédimentaire, avec des caractéristiques à la fois des gisements volcanogéniques de sulfures massifs de type Cu–Zn et Zn–Pb–Cu. Les minéraux du minerai sont la pyrite recristallisée à gros grains, avec sphalérite et chalcopyrite accessoires, galène, arsénopyrite, et minéraux de la série de la tétraédrite. Les minéraux présents en traces sont bornite, marcasite, pyrrhotite, mackinawite, molybdénite, covellite, digénite, chalcocite, gudmundite, boulangerite–bursaïte, kobellite–tintinaïte, ménéghinite, cosalite, magnétite, ilménite, rutile, bismuth natif, et électrum. Les minéraux du minerai et la plupart des oxydes sont considérés syngénétiques avec la Formation de Chopawamsic, d'âge cambrien inférieur, et ont plus tard été recristallisés pendant un épisode de métamorphisme, jusqu'au faciès amphibolite inférieur. Les changements de composition de la phase fluide responsable de la minéralisation après la déposition initiale ont mené à une zonation grossière de Zn/Pb *versus* Cu, et ont probablement causé le remplacement de tétraédrite–freibergite par une intercroissance graphique riche en arsenic et en fer. Un ré-équilibrage plus poussé a mené à l'exsolution dans plusieurs sulfosels, y inclus la tétraédrite–freibergite associée à la galène. Le paroxysme métamorphique semble avoir atteint une température d'environ 470°C, avec une activité du soufre dans l'intervalle –4.5 à –6.3 atmosphères.

(Traduit par la Rédaction)

Mots-clés: gisement de sulfures massifs volcanogéniques, sulfosels, tétraédrite, tennantite, gisement de Cofer, ceinture à pyrite + or, ceinture minéralisée, Virginie.

---

[1] *E-mail address*: jwmiller@unca.edu

INTRODUCTION

The Cofer property lies five kilometers north-northeast of Mineral, Louisa County, in the central Piedmont of Virginia. The property is near the northern end of two convergent northeasterly trending mineralized zones: a western one known for base metals, and the eastern Fisher Lode trend, known for lode-gold prospects (Fig. 1). Mining in the general area dates from the pre-Revolutionary War period (mid-18th century), with at least 20 mines and prospects known from Louisa County alone (Luttrell 1966). The mining had been directed toward pyrite-rich ores for recovery of sulfur, gold, and minor lead and zinc (Table 1). The Cofer deposit is particularly rich in Sb–Bi–As sulfosalts and sulfides that provide clues to the formation and subsequent alteration of the deposit. The purpose of this study is to describe the ore minerals and their textures within the mineralized zones.

TABLE 1. MINING ACTIVITY IN THE GOLD-PYRITE BELT OF VIRGINIA

date	activity	references
1714	gossan mining for iron began	Holden (1905), Poole (1973)
1794	first mention of gold in the southern states	Jefferson (1794)
1831-56, 1930's-40's	gold mining	Sweet (1971), Brown (1937)
1847-65	supergene copper mining	Currier (1935)
1849-1919, 1942-45	zinc and lead mining	Currier (1935), Grosh (1949a, b), Luttrell (1966)
1865-1922	pyrite mined for sulfuric acid + Cu, Pb, Zn	Watson (1907), Lonsdale (1927), Luttrell (1966), Hickman (1947)

The Cofer deposit was discovered through geochemical surveys in the 1960s by The New Jersey Zinc Company (R.F. Kazda, pers. commun., 1978), which entered into a joint venture with Callahan Mining Corporation to form Piedmont Mineral Associates in 1972. In the mid-1970s, Piedmont Mineral Associates explored the Cofer deposit with diamond drilling from the surface and drove drifts at 160- and 340-foot (49- and 104-meter) depths. Four *en échelon* lenses containing a total of approximately 1.5 Mt of ore grading 7% combined Zn and Pb have been defined (Duke & Hodder 1986). Recognition of abundant metamorphosed volcanic rocks in the vicinity of the Cofer deposit and similarities with published accounts of other volcanogenic deposits led Piedmont Mineral Associates geologists to interpret the Cofer as a submarine exhalative deposit.

In 1977, the Cofer deposit was placed on a standby status, and the underground workings were allowed to flood. To date, no ore has been produced at Cofer.

REGIONAL GEOLOGY

The Cofer deposit is located in the Virginia Piedmont physiographic province, with the Blue Ridge province to the west and the Coastal Plain to the east. The Piedmont is characterized by Precambrian to early Paleozoic "eugeosynclinal" rocks that are underlain by Precambrian basement gneiss and intruded by numerous diabase dikes of Triassic age (Fisher 1970). Deep weathering has resulted in formation of a thick saprolite throughout much of the area. Several other nearby massive sulfide deposits with similar mineralogy and the same geological setting were found as gossans over pyrite-rich bodies. These include the Arminius, Sulphur, and Boyd Smith deposits mined for pyrite, and the Julia deposit, which did not produce ore (Fig. 1).

Massive sulfide lenses of the Cofer deposit occur within the Chopawamsic Formation (Fig. 2) (Southwick *et al.* 1971, Gair 1978, Pavlides *et al.* 1982, Sauer 1983, Duke 1983), which probably formed during the Early Cambrian, on the basis of discordant zircon data (Horton *et al.* 1989). Two general ideas have emerged concerning the tectonic interactions that led to the development of the Chopawamsic Formation. The prevailing idea in the late 1970s and 1980s involved the interaction of various microplates with the North American craton in the formation of the Chopawamsic (Hodder *et al.* 1977, Pavlides 1981, Pavlides *et al.* 1982, Williams & Hatcher 1982, Shanmugam & Lash 1982, Duke & Hodder 1986, Drake *et al.* 1989, Horton *et al.* 1989). The origin of the Chopawamsic Formation has been described as part of a tholeiitic island-arc suite with calc-alkaline components (Pavlides 1981, Pavlides *et al.* 1982) and as an immature continental margin – volcanic rift setting (Duke & Hodder 1986). The Chopawamsic Formation, Ta River Metamorphic Suite, and James Run Formation make up the Chopawamsic Terrane, which joined with the Potomac Terrane, probably the Belair – Rising Sun, and perhaps other exotic terranes during the Penobscottian orogeny (550–490 Ma). Then, these terranes and others, such as the Carolina terrane, were joined to Laurentia during the Taconic Orogeny (470–440 Ma) (Drake *et al.* 1989, Horton *et al.* 1989). A more recent account (Dalla Salda *et al.* 1992a, b, Dalziel *et al.* 1994, Dalziel 1997) invoked the cessation of synrift magmatism at the latest Precambrian. At the Precambrian–Cambrian boundary, Gondwana and Laurentia began rifting, with a gap at their southern boundary occupied by the Texas plateau that originated from the Cape of Good Hope embayment within Gondwana. By Middle Ordovician, the proto-Appalachian and proto-Andean margins converged, and ultimately collided during the Taconic orogeny, separated by the Texas Plateau, Precordillera, and possibly the Carolina Terrane.

Duke (1983) subdivided the Chopawamsic into a western section of felsic pyroclastic rocks, a central section of bimodal metavolcanic rocks within thick epiclastic metasedimentary units intruded by felsic plutons, and an eastern section of amphibolitic metabasalt. The eastern section reached the greenschist facies, and the central section attained greenschist- to amphibolite-facies metamorphism (Duke 1983, Duke & Hodder 1986). Sandhaus & Craig (1986) estimated that the Chopawamsic in the study area reached 470°C,

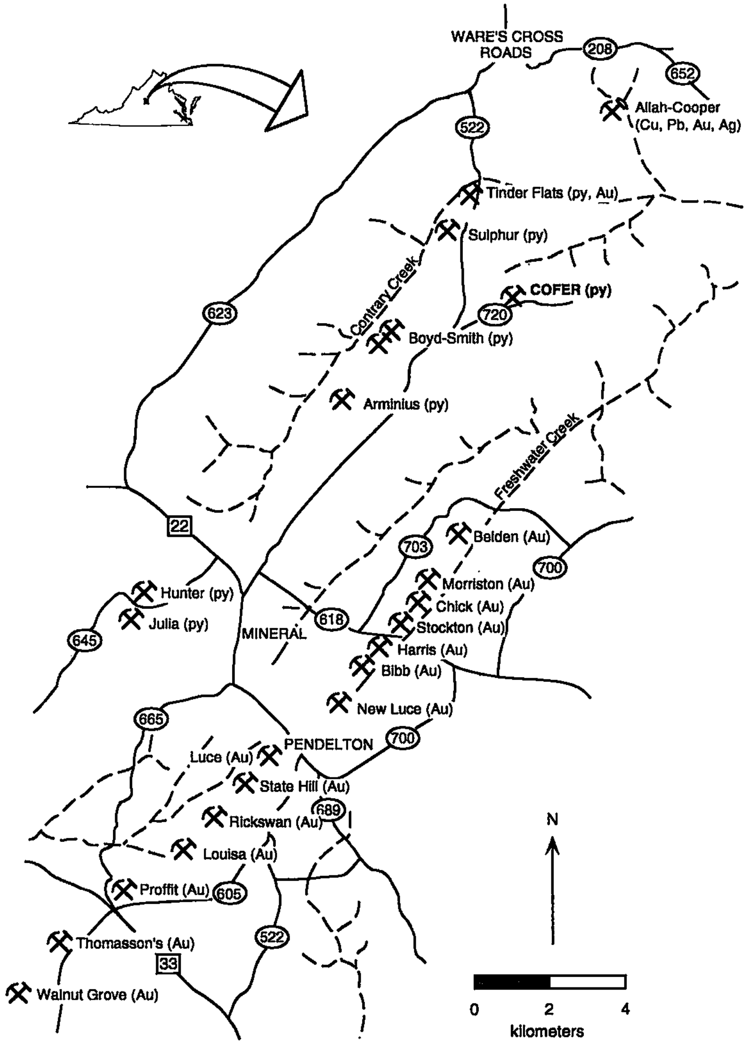

FIG. 1. The Gold–Pyrite Belt of Virginia, showing the location of the Cofer deposit.

on the basis of Fe/Mg distribution coefficients between garnet and biotite, and 3 kbar, on the basis of FeS content of sphalerite in equilibrium with pyrite and pyrrhotite. Massive sulfides occur in the central section and are interpreted as a rift metallotect (Duke & Hodder 1986).

Four major lenses of massive sulfide at the Cofer deposit have been identified: hanging wall, Cofer, footwall, and distal footwall (Fig. 3). Two minor lenses have been delineated: the "distal–distal footwall" and "hanging wall – hanging wall." According to Hodder *et al.* (1977), these *en échelon* lenses are stratabound and "conformable to semi-conformable to foliation", with an average attitude of N33°E, 65°SE. Original sedimentary features, such as primary sulfide banding and volcanic fragmental textures, were preserved at the Cofer deposit, even though metamorphism had reached lower amphibolite facies (Hodder *et al.* 1977) (Fig. 4). Opaque minerals at Cofer are primarily pyrite with sphalerite and minor chalcopyrite, galena, arsenopyrite, and tetrahedrite–tennantite-series minerals, hereafter referred to as the tetrahedrite series. Minerals in trace amounts include bornite, marcasite, pyrrhotite, mackinawite, molybdenite, covellite, digenite, chalcocite, gudmundite, meneghinite, boulangerite–bursaite, kobellite–tintinaite, cosalite, magnetite, ilmenite, rutile, electrum, and native bismuth.

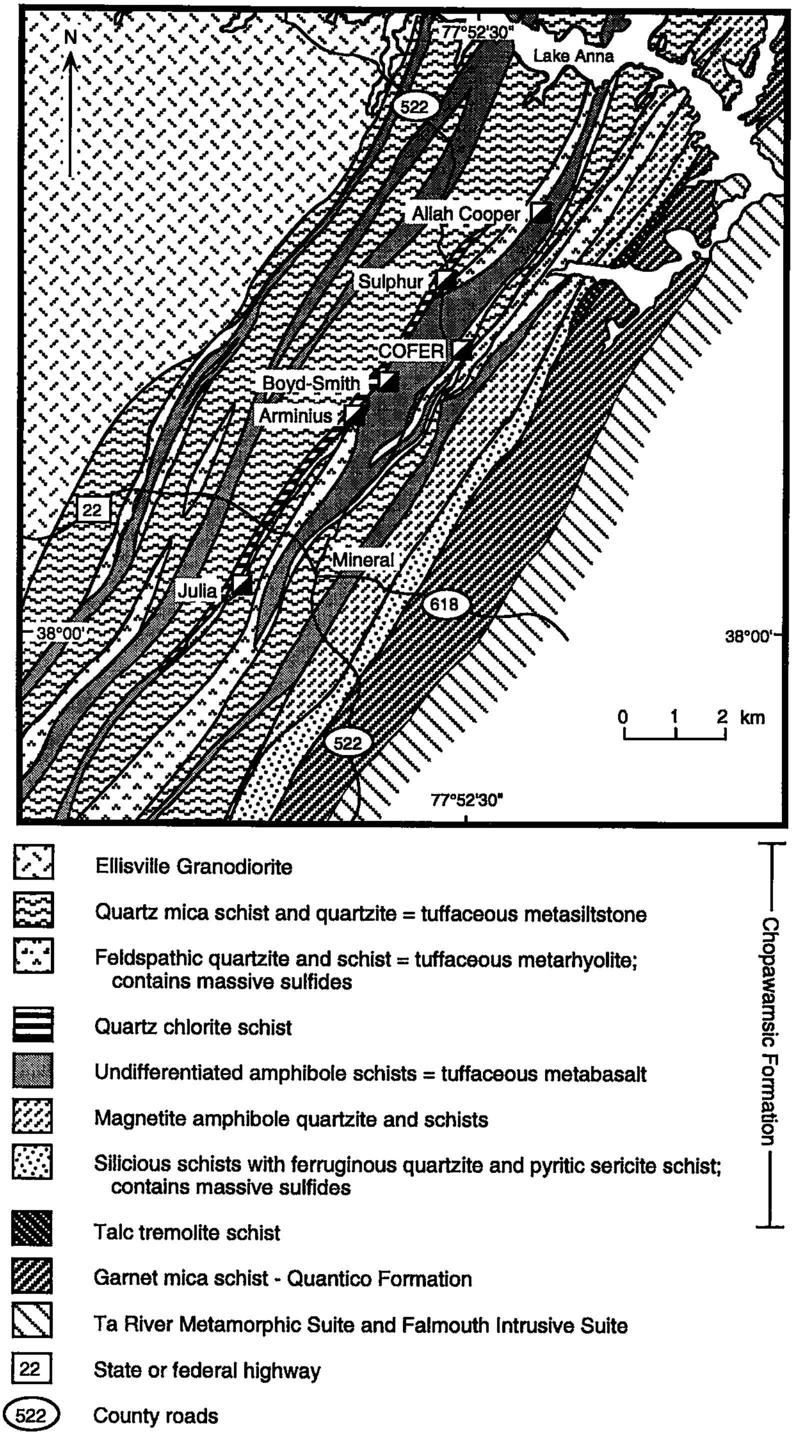

FIG. 2. Geological map of the Mineral District, Louisa County, Virginia. After Sauer (1983) and Duke & Hodder (1986).

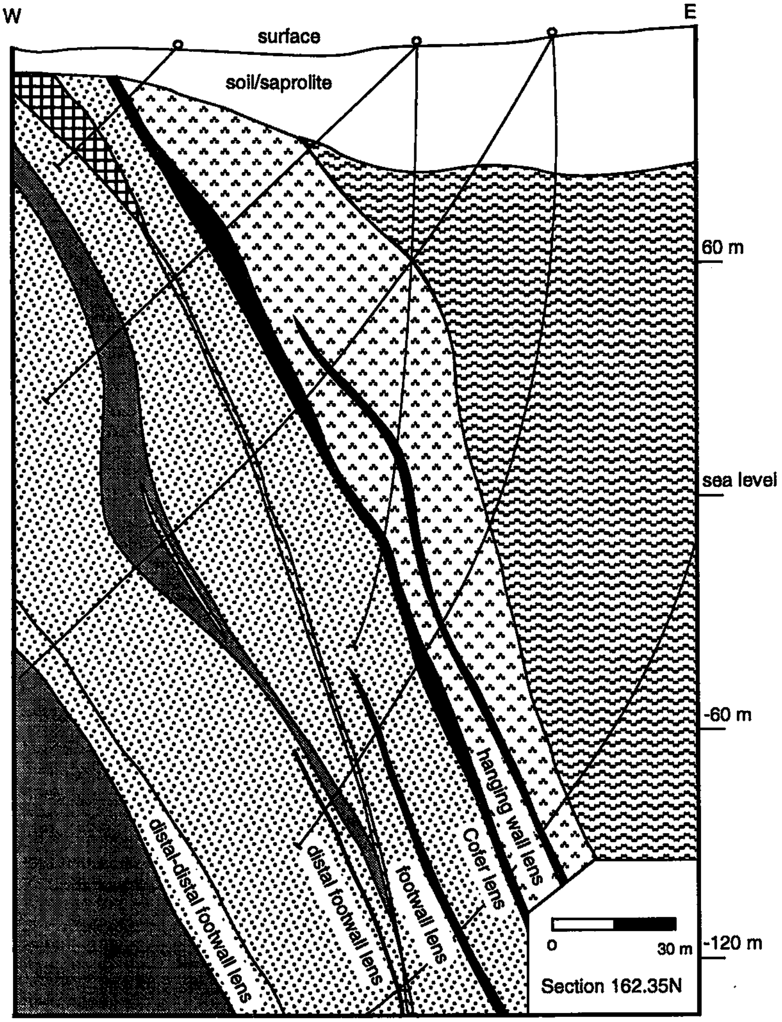

FIG. 3. The Cofer deposit, cross section looking N34°W. After Hodder *et al.* (1977) and Duke & Hodder (1986). Patterns of the various units correspond to those of Figure 2, except for the cross-hatching, which represents metagraywacke – crystal lithic tuff.

ZONING IN "ORE" AND ORE MINERAL

The ores of Cofer may be grouped into four major types: (1) yellow ore, (2) black ore, (3) pyrite ore, and (4) disseminated ore. These terms are now well established in the literature of volcanogenic sulfide deposits and thus are used to designate mineralogical makeup and texture (*e.g.*, Sato 1974, Eldridge *et al.* 1983).

(1) Yellow ore is similar to *oko* (yellow ore) of Kuroko-type deposits. It consists of coarse, subhedral to euhedral pyrite (75% by volume), with interstitial chalcopyrite and minor or trace arsenopyrite, molybdenite, and boulangerite. Also occurring in yellow ore at Cofer is a graphic intergrowth (referred to hereafter as "the graphic intergrowth") of arsenopyrite and chalcopyrite ± tetrahedrite-series minerals ± other minor minerals.

(2) Black ore, similar to *kuroko* (black ore) of Kuroko-type deposits, consists of subequal amounts of sphalerite and euhedral to subhedral pyrite, with smaller amounts (5 to 10 vol.%) of galena and chalcopyrite, and minor gangue. Locally, black ore may consist entirely of massive sphalerite with local concentrations of galena or chalcopyrite (or both). Cosalite, boulangerite, bursaite, meneghenite, and tetrahedrite-series minerals occur also in black ore at Cofer.

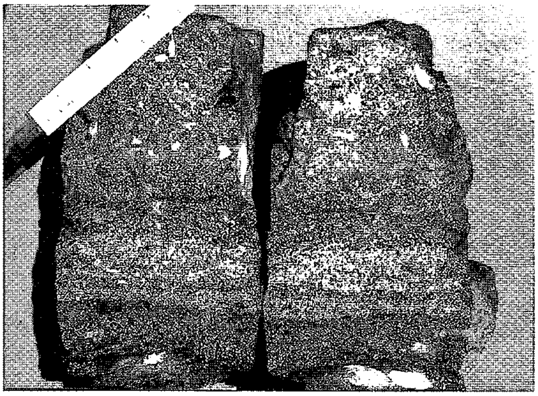

FIG. 4. Cofer ore (pyrite, gangue), showing original sedimentary layering. Major subdivisions on the ruler are inches on top and centimeters on the bottom.

(3) Pyrite ore at Cofer is similar to *ryukako* (pyrite ore) of Kuroko deposits and consists of pyrite with trace amounts of sphalerite, chalcopyrite, galena, and silicates.

(4) Disseminated ore, similar to *keiko* or *keishitsuko* (siliceous ore) at Kuroko deposits, chiefly contains quartz and muscovite, with lesser amounts of biotite, chlorite, calcite, plagioclase, and K-feldspar. The ore minerals occur as small, widely dispersed grains of pyrite, sphalerite, chalcopyrite, and galena. Chalcopyrite also occurs as infrequent fracture-fillings up to several centimeters across within cross-cutting lenticular veins of quartz.

"Ore" types at Cofer may exist also as variations that are transitional between the four categories described above. The ore types, in order of decreasing abundance, are disseminated ore, pyrite ore, black ore, and yellow ore. Distinct zoning of the deposit is not evident, but trends of ore-type abundance are well defined. Black ore is dominant at the southwestern end of the Cofer deposit, and pyrite-disseminated ore is dominant toward the northeastern end (Fig. 5).

OPAQUE MINERALS

Minerals from Cofer were obtained by systematic sampling of drifts and drill core, and were identified by optical methods, energy-dispersion analysis, and electron-microprobe analysis. Methods are described in Appendix I.

Pyrite is the most abundant ore mineral in all ore types at Cofer. The composition is stoichiometric, except for trace amounts of arsenic that are indicated by X-ray imaging (Fig. 6), and are below the detection limit for chemical analysis (0.02 wt.%). Neither cobalt nor nickel were detected (<0.02 wt.%). Pyrite is typically dispersed as subhedral cubes (≤1 mm), which are less commonly anhedral or euhedral. It may be disseminated or in polycrystalline masses. Pyrite may exhibit an annealed texture, showing somewhat rounded grains with 120° dihedral angles, especially where it occurs in pyrite ore. Although most grains of pyrite appear featureless, some contain a concentric growth-zoning defined by fine-grained inclusions of gangue particles (Fig. 6a) that may be made much more visible by etching with nitric acid or hydrogen peroxide (Fig. 6b). The growth pattern is paralleled by subtle zoning in arsenic, revealed by electron-microprobe mapping (Fig. 6c). Some sections show an overgrowth, with core and rim of different relief and different etch patterns. Energy-dispersion and wavelength-dispersion spectrometers have indicated no consistent compositional variation in the overgrowths. Relief after polishing appears to be a result of an anisotropy in hardness corresponding to differences in crystallographic orientation. No colloform or framboidal textures occur at Cofer. Inclusions are common, and dominantly composed of coexisting sulfides, such as sphalerite, chalcopyrite, galena and, less commonly, arsenopyrite, pyrrhotite, and tetrahedrite-series minerals. Quartz, K-feldspar, calcite, and rutile occur also as inclusions in pyrite. The inclusions mostly fall into two textural groups: (1) round, annealed inclusions, and (2) irregular inclusions.

Sphalerite is ubiquitous but highly variable in amount in the massive sulfides. It may occur in layers (≤3 mm in thickness), or in disseminated anhedral grains (≤1 mm). Sphalerite commonly displays recrystallization-induced twinning and is optically and chemically homogeneous. Chalcopyrite is present as sparse, randomly oriented and dispersed inclusions in many grains of sphalerite. Locally, chalcopyrite inclusions are abundant and may occur in rows that are crystallographically controlled. This texture, referred to as "chalcopyrite disease", likely results from replacement of iron-bearing sphalerite by chalcopyrite and low-iron sphalerite during mineralization, or by epitactic growth of chalcopyrite during formation (Hutchison & Scott 1979, Wiggins & Craig 1980, Barton & Bethke 1987). Rare textures in sphalerite include skeletal growths (stars) of sphalerite in chalcopyrite (Fig. 7) and an intergrowth of tennantite in sphalerite resembling the flame structures found in the Sudbury nickel ores. At Cofer, sphalerite contains widely varying amounts of iron and significant amounts of cadmium and manganese (Table 2).

Galena occurs generally as small disseminations (≤1 mm), but locally is found in grains up to one cm across. It is sparse in pyrite ores, but its abundance markedly increases with the increase of sphalerite in black ores. Galena commonly contains as much as 0.2 wt.% Ag and 0.5% Bi (Table 2). Sulfosalt inclusions are common in galena and include tetrahedrite, freibergite, boulangerite, and native bismuth.

Chalcopyrite occurs in disseminated anhedral grains (≤0.5 mm), as inclusions in pyrite and sphalerite, and in polycrystalline masses that may reach several cm in quartz veins. Chalcopyrite is nearly ubiquitous and displays broad, lamellar twinning. Mackinawite, sphalerite, galena, molybdenite, kobellite, boulangerite, electrum, and the graphic intergrowth occur as inclusions in chalcopyrite. Locally, alteration of chalcopyrite by groundwater has resulted in the formation of bornite, covellite, digenite, and chalcocite.

All other ore minerals occur in minor or trace amounts. *Bornite* appears only in a few sections as small (≤0.05 mm), mutually parallel and elongate lamellae intergrown with covellite, with the resulting texture included in chalcopyrite. *Marcasite* altered to pyrite occurs as dispersed grains (≤0.5 mm) in massive to disseminated sulfide sections. It is porous and displays parallel lamellar zebra-like twin domains in some sections. Marcasite is stoichiometric and contains inclusions of calcite and silicate. In disseminated ore, some large crystals of garnet (≤5 mm) contain a core of marcasite. *Pyrrhotite* coexists as round inclusions (≤0.01 mm) with chalcopyrite (± sphalerite, rarely + arsenopyrite) in host pyrite and rarely as a single-phase inclusions (≤0.05 mm) in chalcopyrite, pyrite, galena, or the graphic intergrowth. *Mackinawite* (FeS_{1-x}) exists as tiny, scattered, worm-like blebs (≤0.005 mm) in twinned chalcopyrite. These blebs are optically but not spatially oriented (Fig. 8). Electron-microprobe analysis revealed the presence of only iron, copper, and sulfur. *Molybdenite* occurs at Cofer in trace amounts as platelets (0.01–0.1 mm) associated with chalcopyrite or sphalerite in yellow ore and pyrite ore. Molybdenite may be locally abundant in association with or included in pyrite and quartz. Electron-microprobe analysis revealed only molybdenum and sulfur. The copper sulfides *covellite* (CuS), *digenite* [$(Cu,Fe)_9S_5$], and *chalcocite* (Cu_2S) occur in trace amounts as stringers and rims around chalcopyrite, tetrahedrite-series minerals, and galena.

Sulfarsenides and sulfantimonides are widespread at the Cofer deposit. *Arsenopyrite* occurs in three distinct associations: (1) euhedral and subhedral rhombohedra (≤0.5 mm) associated with tennantite and chalcopyrite, (2) subhedral and anhedral grains (≤2 mm) associated with pyrite, and (3) subhedral to euhedral rhombohedra (≤0.5 mm) that form an integral part of the graphic intergrowth (Fig. 9). Arsenopyrite commonly displays a complex hourglass type of optical zoning, and contains no detectable cobalt or nickel. *Gudmundite* (FeSbS) exists as rare, small (≤0.05 mm), subhedral to anhedral grains as part of the graphic intergrowth in yellow ore. *Tetrahedrite-series minerals* occur in all but the distal footwall lens at Cofer, and they are found in all ore types, but are concentrated in black ore. The tetrahedrite-series minerals span the entire range between end-members tennantite ($Cu_{12}As_4S_{13}$), tetrahedrite ($Cu_{12}Sb_4S_{13}$), and freibergite [$(Cu,Ag)_{12}Sb_4S_{13}$], and are described in detail by Miller & Craig (1983). These minerals have an average composition of $(Cu,Ag,Fe,Zn)_{11.9}(As,Sb,Bi)_{4.0}S_{12.4}$ (Table 3), which was normalized to four atoms of the semimetals, as suggested by Seal *et al.* (1990). Freibergite contains in excess of 99% of the total silver content of the Cofer ores, with individual grains containing as much as 29.5 wt.% Ag. Small grains of freibergite and tetrahedrite near (≤1 mm) or included (≤0.05 mm) in galena most likely account for a consistent silver–lead correlation from assay data at Cofer (R.F. Kazda, pers. commun., 1978). The Ag content of galena is ≤0.2%. Miller & Craig (1983) noted the strong correlation of the Ag with the Sb content of the tetrahedrite-series minerals, where the silver-bearing antimony-rich tetrahedrite occurs with a wide variety of other phases, and the silver-deficient arsenic-rich members are associated with arsenopyrite or chalcopyrite or both (Fig. 10). Intermediate tetrahedrite-series minerals may be associated with either galena, or arsenopyrite and chalcopyrite. Bismuth is present in nearly all tetrahedrite-series minerals observed (0.27 wt.% on average) and may reach over 2 wt.%. All grains analyzed from Cofer were found to be chemically homogeneous.

The graphic intergrowth (≤2 mm) (Fig. 9) of sulfides and sulfosalts (Miller & Craig 1983) occurs in yellow ore and is composed of rhombs or irregular grains of arsenopyrite, rounded grains of sphalerite and freibergite–tetrahedrite. Other minerals that may be present include gudmundite, native bismuth, kobellite, pyrrhotite, and galena. The bulk composition of the graphic intergrowth is $(Cu,Ag)_{3.4}(Fe,Zn)_{6.7}Pb_{.05}(As,Sb,Bi)_{4.0}S_{10.1}$ (Table 3), which was obtained by point-counting photographic mosaics of several intergrowths and normalizing to 4.0 atomic units As + Sb + Bi.

Several grains of sulfosalt corresponding to the boulangerite–bursaite series [$Pb_5(Sb,Bi)_4S_{11}$] have been observed in samples from the Cofer deposit. Antimonian and intermediate samples of this series occur in galena or chalcopyrite and may contain exsolved native bismuth. The only case of stoichiometric bursaite analyzed, however, occurs in sphalerite. All examples of boulangerite and bursaite occur as lamellae or elongate blebs (≤0.2 mm). The kobellite–tintinaite series, ideally $Pb_5(Bi,Sb)_8S_{17}$, occurs as small (≤0.1 mm), dispersed grains in the graphic intergrowth and in chalcopyrite in yellow ore (Fig. 9). This rare mineral is associated with freibergite and native bismuth. Kobellite–tintinaite contains approximately equal amounts of antimony and bismuth, and as much as 2 wt.% Cu or Fe or both (Table 2). Rare irregular grains (≤ 0.5 mm) of cosalite ($Pb_2Bi_2S_5$) of stoichiometric composition associated with galena and chalcopyrite were found in one sample of pyrite ore. Meneghinite ($CuPb_{13}Sb_7S_{24}$) occurs as elongate blebs (0.05 × 0.2 mm) in galena and was found in one sample of pyrite ore, also.

Oxide minerals are also common at the Cofer deposit. Magnetite occurs in the wallrock within

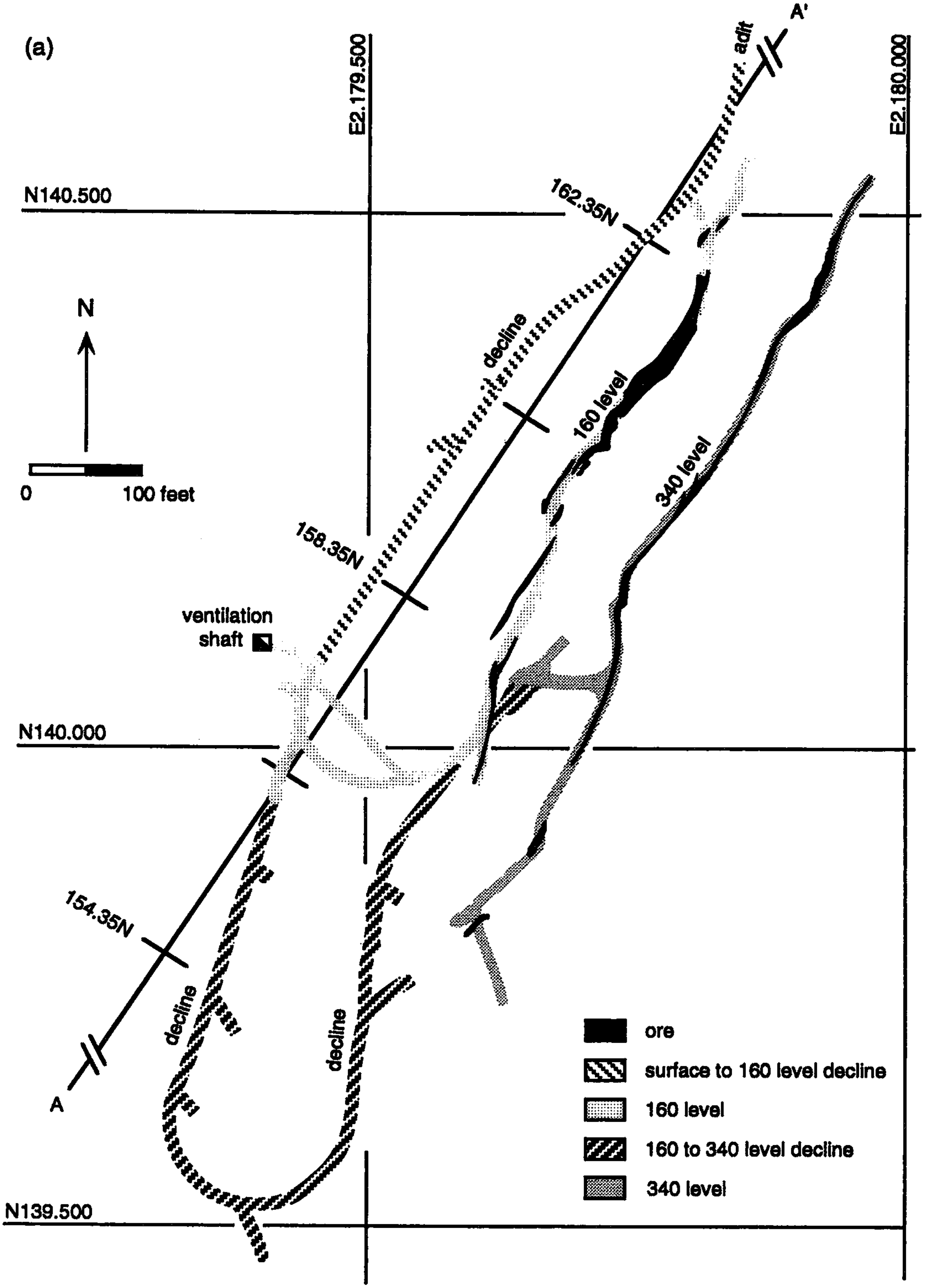

FIG. 5. (a) The Cofer deposit, plan view (courtesy of Callahan Mining Corporation). (b) Ore samples in diamond drill holes (schematic). Duplicate numbers indicate multiple samples taken within that foot of drill core.

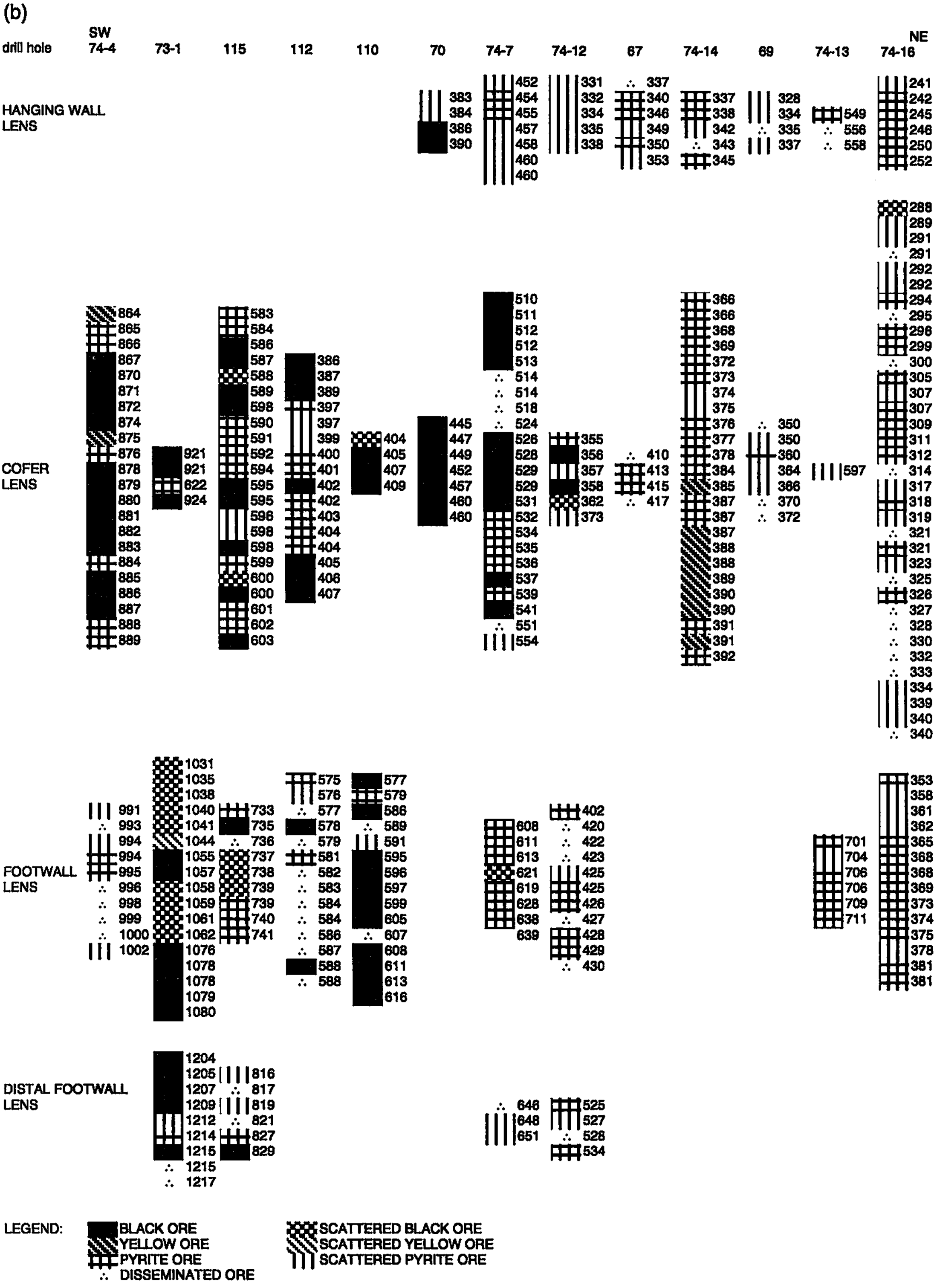
(b)
SW
NE
drill hole
74-4
73-1
115
112
110
70
74-7
74-12
67
74-14
69
74-13
74-16
HANGING WALL LENS
383 384 386 390
452 454 455 457 458 460 460
331 332 334 335 338
337 340 346 349 350 353
337 338 342 343 345
328 334 335 337
549 556 558
241 242 245 246 250 252
COFER LENS
864 865 866 867 870 871 872 874 875 876 878 879 880 881 882 883 884 885 886 887 888 889
921 921 622 924
583 584 586 587 588 589 598 590 591 592 594 595 595 596 598 598 599 600 600 601 602 603
386 387 389 397 397 399 400 401 402 402 403 404 404 405 406 407
404 405 407 409
445 447 449 452 457 460 460
510 511 512 512 513 514 514 518 524 526 528 529 529 531 532 534 535 536 537 539 541 551 554
355 356 357 358 362 373
410 413 415 417
366 366 368 369 372 373 374 375 376 377 378 384 385 387 387 387 388 388 389 390 390 391 391 392
350 350 360 364 366 370 372
597
288 289 291 291 292 292 294 295 296 299 300 305 307 307 309 311 312 314 317 318 319 321 321 323 325 326 327 328 330 332 333 334 339 340 340
FOOTWALL LENS
991 993 994 994 995 996 998 999 1000 1002
1031 1035 1038 1040 1041 1044 1055 1057 1058 1059 1061 1062 1076 1078 1078 1079 1080
733 735 736 737 738 739 739 740 741
575 576 577 578 579 581 582 583 584 584 586 587 588 588
577 579 586 589 591 595 596 597 599 605 607 608 611 613 616
608 611 613 621 619 628 638 639
402 420 422 423 425 425 426 427 428 429 430
701 704 706 706 709 711
353 358 361 362 365 368 368 369 373 374 375 378 381 381
DISTAL FOOTWALL LENS
1204 1205 1207 1209 1212 1214 1215 1215 1217
816 817 819 821 827 829
646 648 651
525 527 528 534
LEGEND:
BLACK ORE
YELLOW ORE
PYRITE ORE
DISSEMINATED ORE
SCATTERED BLACK ORE
SCATTERED YELLOW ORE
SCATTERED PYRITE ORE

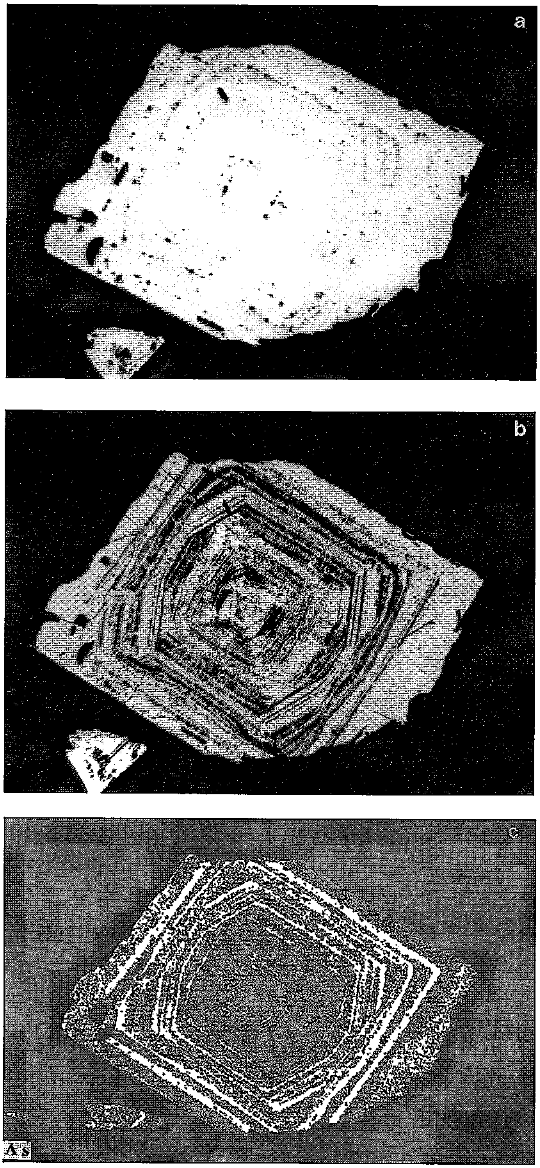

FIG. 6. Pyrite (sample 74–18/602.5; 1.6 mm across grain) showing concentric growth zoning: a) inclusions in plane polarized light, b) sample etched in H_2O_2 for 20 minutes, c) arsenic X-ray image.

FIG. 7. Skeletal growth (stars) of sphalerite in chalcopyrite. Sample from 340 level, field of view: 0.45 mm.

biotite–magnetite schist and amphibolite, but only three sulfide samples observed within two meters of each other in the Cofer lens contain magnetite. Magnetite grains are rounded (~0.5 mm across) and homogeneous. Iron is the only cation present. The relative paucity of magnetite in the Cofer ore contrasts with ores from the nearby Arminius and Sulphur mines, where magnetite is abundant within sulfide bodies. Ilmenite occurs in some samples as rounded grains (≤0.05 mm) in quartz and micas at Cofer. Rutile occurs in many samples as tiny inclusions (≤0.005 mm) in pyrite and as rounded grains (≤0.05 mm) in some quartz and mica. Single needles (≤0.05 mm) of rutile occur rarely in sphalerite.

Native elements are widespread as inclusions in sulfide minerals. Electrum (Au,Ag) occurs rarely as flecks (≤0.005 mm) in chalcopyrite, and is the only auriferous phase at the Cofer deposit. Probably less than 1% of the silver from Cofer is contained in electrum; the rest is in the freibergite. The largest grain observed (0.01 mm) has a ratio of 56:43 gold to silver in weight % (41:59 Au:Ag in atomic proportions). Native bismuth occurs as minute (≤0.005 mm) and in some places larger (≤0.1 mm) roundish inclusions in galena, boulangerite, and kobellite. The inclusions contain approximately 1.2 wt.% Sb (Table 2), possess lamellar twins, and are associated with arsenopyrite, tetrahedrite-series minerals, chalcopyrite, and the graphic intergrowth. Native bismuth that occurs as inclusions in galena has been observed only in the hanging wall and Cofer lenses, whereas intergranular native bismuth is concentrated in yellow ore in the Cofer lens.

EFFECTS OF METAMORPHISM

The Cofer deposit is located within a sequence of metasedimentary and metavolcanic rocks that have been metamorphosed to greenschist and amphibolite facies (Sandhaus & Craig 1986, Duke & Hodder 1986). Typical mineral assemblages (garnet, chlorite,muscovite, plagioclase) exist in the ore and the wallrock, and indicate that both units have been subjected to amphibolite-facies metamorphism. Although much of the Virginia Piedmont is characterized by intense

TABLE 2. RESULTS OF ELECTRON-MICROPROBE ANALYSES, SULFIDES AND SULFOSALTS FROM THE COFER DEPOSIT

	Cu	Ag	Fe	Zn	Pb	As	Sb	Bi	S	Total
boulangerite-bursaite										
69/334	-	-	-	-	55.8	0.4	24.1	2.4	18.6	101.3
70/451.5	0.2	0.02	0.1	0.4	58.3	0.4	21.3	1.0	16.9	98.6
73-1/921	1.2	-	-	-	51.3	0.1	17.0	13.4	18.3	101.3
73-1/920.5	-	0.4	0.4	0.1	53.0	0.2	13.3	15.7	17.0	100.1
74-14/387.4-2	1.0	0.1	0.5	-	50.2	-	9.9	22.2	16.9	100.8
74-4/871	0.4	-	0.02	-	57.8	0.02	7.6	17.6	15.7	99.1
73-1/1205	-	0.7	0.2	3.1	47.0	-	0.3	35.8	16.1	103.2
kobellite-tintinaite										
74-14/391.3	1.4	0.3	0.6	-	33.9	0.1	12.2	32.6	17.8	98.1
74-14/389.7	0.5	0.04	1.9	-	38.4	-	13.7	26.3	18.5	99.3
74-14/387.4	1.8	-	1.5	-	39.2	-	17.9	20.9	18.9	100.2
cosalite										
115/598.4	4.0	0.2	0.6	0.1	39.0	-	0.4	39.7	16.8	100.8
meneghinite										
74-12/356.8	1.3	-	0.1	-	59.7	-	15.5	7.6	17.0	101.2
gudmundite										
74-14/391.3	4.9	-	27.4	-	0.1	1.7	48.9	1.0	17.4	101.4
74-14/391.3-2	1.7	0.02	27.2	0.2	0.2	2.2	53.0	0.8	15.9	101.2
galena										
70/449	-	0.3	0.3	-	88.0	-	-	-	13.6	102.2
74-14/388.9	0.2	0.2	0.3	-	85.1	-	-	1.3	13.6	100.7
native bismuth										
74-14/391.3	1.0	0.1	0.6	1.4	0.3	0.03	1.2	95.1	0.1	99.8

* Individual tetrahedrite series analyses are published in Miller and Craig (1983)

Average Standard Deviations

Boulangerite-bursaite Cu: 0.3; Ag: 0.1; Fe: 0.1; Zn: 0.3; Pb: 0.4; As: 0.04; Sb: 0.4; Bi: 0.3; S: 0.2
Kobellite-tintinaite Cu: 0.2; Ag: 0.04; Fe: 0.2; Pb: 0.4; As: 0.04; Sb: 0.6; Bi: 0.9; S: 0.2
Cosalite Cu: 0.1; Ag: 0.1; Fe: 0.03; Zn: 0.1; Pb: 0.5; Sb: 0.02; Bi: 0.1; S: 0.2
Meneghinite Cu: 0.6; Ag: 0.01; Fe: 0.1; Zn: 0.04; Pb: 0.6; As: 0.1; Sb: 1.0; Bi: 0.3; S: 0.1
Gudmundite Cu: 0.7; Ag: 0.05; Fe: 0.2; Pb: 0.2; Bi: 0.2; S: 0.02
Galena Cu: 0.7; Ag: 0.05; Fe: 0.2; Pb: 0.2; Bi: 0.2; S: 0.02
Native Bismuth Cu: 0.1; Ag: 0.02; Fe: 0.03; Pb: 0.05; As: 0.01; Sb: 0.04; Bi: 0.7; S: 0.01

TABLE 2 (continued). RESULTS OF ELECTRON-MICROPROBE ANALYSES, SULFIDES AND SULFOSALTS FROM THE COFER DEPOSIT

	Fe	As	S	Total
arsenopyrite				
74-4/882	34.5	44.0	20.5	99.0
74-4/866	35.3	43.7	21.0	100.0
115/587.5	34.0	45.0	20.4	99.4
115/588.8	34.5	43.9	20.8	99.2
115/590.3	33.9	44.9	21.0	99.8
115/595.9	35.0	44.2	20.7	99.9
115/737.9	33.7	44.1	20.8	98.6
115/738.8	34.2	44.7	20.3	99.2
112/401.5	35.1	44.2	20.7	100.0
112/402	34.3	45.1	20.5	99.9
112/405.5	33.5	45.0	20.6	99.1
110/613	33.9	44.7	20.6	99.2
110/616	33.3	46.3	19.2	98.8
74-7/526.2	35.1	44.1	21.1	100.3

*Average Standard Deviations
Fe: 0.3; As: 0.3; S: 0.3

TABLE 2 (continued). RESULTS OF ELECTRON-MICROPROBE ANALYSES, SULFIDES AND SULFOSALTS FROM THE COFER DEPOSIT

	Cu	Fe	Zn	Mn	Cd	S	Total	Mole% FeS
sphalerite								
73-1/1057	0.1	2.4	67.6	0.04	0.2	32.4	102.7	4.1
73-1/1204	0.02	4.6	63.4	0.02	0.2	33.2	101.4	7.9
73-1/1206.5	0.2	3.6	63.7	0.02	0.2	33.2	100.9	6.2
73-1/1216.8	0.1	6.9	62.1	0.1	0.3	32.3	101.8	11.8
115/828.5	0.1	11.0	55.8	0.04	0.7	33.7	101.3	18.7
112/402	0.7	2.1	64.7	0.1	0.3	33.2	100.9	3.6
70/446.6	0.04	4.5	62.1	0.02	0.2	34.0	100.9	7.7
70/451.5	0.1	6.9	62.1	0.1	0.3	32.3	101.8	11.8
74-12/334	0.1	8.6	59.0	0.2	0.3	32.6	100.8	14.8
67/345.6	-	6.3	61.0	0.1	0.2	31.8	99.4	11.1
67/349	0.03	5.5	61.1	0.1	0.2	33.2	100.1	9.5
67/415	0.04	7.6	60.3	0.03	0.2	32.8	101.0	13.1
69/334	0.04	6.7	61.5	-	0.2	33.0	101.4	11.5
69/350	0.01	6.2	60.4	0.1	0.1	33.1	99.9	10.7

Average Standard Deviations
Cu: 0.07; Mn: 0.03; Cd: 0.1; Fe: 0.1; Zn: 0.4; S: 0.4

folding and faulting, ores at the Cofer deposit exhibit little deformation. Indeed, long axes of lithic clasts and mineral grains are not necessarily parallel to compositional layering or foliation (B.A. Bouley, pers. commun., 1993). The rocks exposed along Contrary Creek and in the decline and drifts of the Cofer deposit dip homoclinally to the southeast at an average of 65° (Hodder *et al.* 1977). No folding is apparent, although crenulation cleavage is evident along Contrary Creek to the north and in drill core from the Arminius mine to the southwest. A few contorted zones in the ore at Cofer have been interpreted as primary soft-sediment slump structures (R.W. Hodder & R.F. Kazda, pers. commun., 1976). Cross-cutting fractures filled with white to clear quartz appear to be tensional features. These fractures contain small amounts of chalcopyrite, which may have resulted from the scavenging action of fluids remobilized during metamorphism.

Although the ores of the Cofer property show little evidence of dynamic metamorphism, they have been extensively recrystallized as a result of thermal metamorphism. Thin films and small grains of chalcopyrite that adhere to crystal outlines of pyrite were interpreted by Mookherjee (1976) to be a product of thermal metamorphism. However, the refractory nature of the pyrite commonly allows preservation of premetamorphic textures (Craig & Vokes 1993) such as original growth-zoning, which is shown in pyrite at Cofer by concentric trace amounts of arsenic, rarely by concentric patterns of inclusions, and patterns made apparent by etching (Fig. 6). In many instances, pyrite is found elongated parallel to the schistosity of the enclosing rocks; these grains of pyrite show concentric zoning also, such that the elongation likely is due to growth and not deformation. Moreover, inclusions within pyrite tend to be equant and round, and show no preferred orientation that may be indicative of

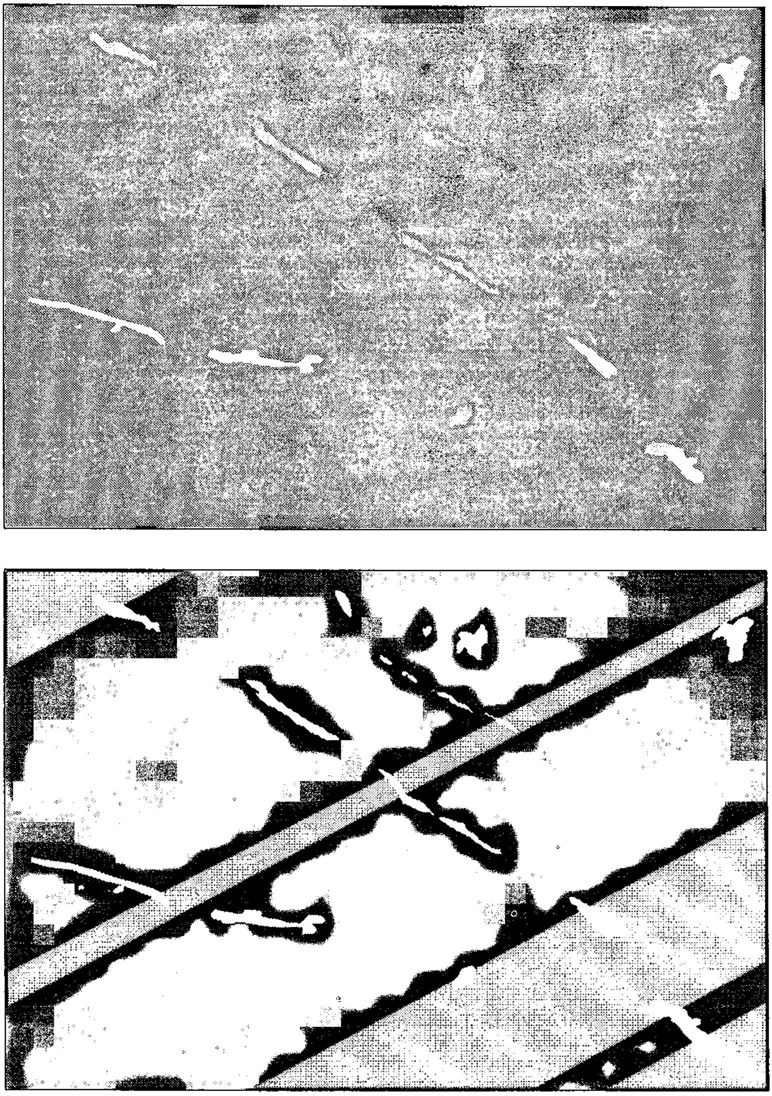

FIG. 8. Optically oriented mackinawite with sphalerite in chalcopyrite; (a) plane-polarized light, (b) crossed nicols. Sample 74–14/388.9, field of view: 0.45 mm.

deformation. Only a few, rare grains of pyrite contain fractures filled with chalcopyrite; the vast majority of pyrite grains show no evidence of cataclasis.

Broad lamellar twinning is evident in sphalerite at Cofer, but the twins show no preferred orientation, such as parallel deformation-induced twins caused by dynamic metamorphism (Vokes 1969). Twinning in sphalerite at Cofer is interpreted as simple recrystallization-induced twinning, like that described by Richards (1966) in the Broken Hill ores. Effects of thermal metamorphism in sphalerite and tetrahedrite-series minerals include optical and chemical homogeneity. These minerals are zoned in many volcanogenic deposits that have experienced only low grades of metamorphism (*e.g.*, Yui 1970, Shimazaki 1974). Although the grains of sphalerite and tetrahedrite-series minerals are compositionally homogeneous, the proportions of iron in sphalerite and cation proportions in tetrahedrite-series minerals vary greatly from one grain to another (Table 2, Miller & Craig 1983). The homogeneous grains of sphalerite and tetrahedrite-series minerals, the wide compositional variation among grains, along with preservation of original sedimentary layering, are indicative of equilib-

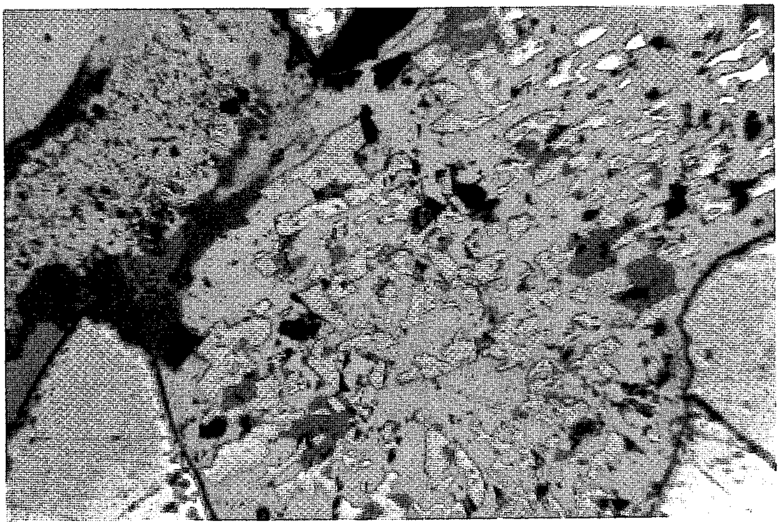

FIG. 9. Graphic intergrowth. Arsenopyrite, chalcopyrite, sphalerite, tetrahedrite, native bismuth, and pyrite. Sample 74–14/391.3; field of view: 0.45 mm.

rium over small domains. The size of these domains is probably on the order of millimeters, as described by Stanton (1976) and Scott *et al.* (1977) at the Broken Hill deposit in Australia, and by Kase (1977) at the Besshi deposits in Japan.

Galena from the Cofer deposit shows no sign of deformation, such as curved cleavage, kink bands, partings, or microfractures, like those features described by Salmon *et al.* (1974) in their study of deformation of galena. Most likely, the thermal metamorphism that homogenized the sphalerite and tetrahedrite-series minerals was responsible for annealing and obliteration of any prior deformational features in galena. This thermal metamorphism apparently resulted in the remobilization of some galena that became incorporated as abundant inclusions in pyrite. Galena occurs uncommonly in fractures, but has not been observed in pressure shadows of other minerals.

COMPARISON WITH OTHER VOLCANOGENIC DEPOSITS

Various classifications of volcanogenic massive sulfide deposits have been presented, including those by Hutchinson (1973), Sawkins (1976), Solomon (1976), Sangster & Scott (1976), Large (1977), Franklin *et al.* (1981), and Morton & Franklin (1987). The most recent classification (Franklin 1990) divides these deposits into the Cu–Zn and Zn–Pb–Cu groups. The Cofer deposit is similar to Cu–Zn deposits by juxtaposition to mafic metavolcanic rocks, by having a tabular, concordant shape, and by lacking any nearby domal eruptive center. On the other hand, Cofer resembles Zn–Pb–Cu ores by lacking a well-defined stringer (stockwork) zone underlying the mineralized bodies, by its metal zoning, and by its metal composition. No stringer zone has been identified at base-metal deposits in the Mineral District except near the Julia deposit, which is stratigraphically 900 meters below the Cofer (Pavlides *et al.* 1982). Metal zoning, albeit lateral rather than vertical, is akin to the Zn–Pb–Cu group, and so are the overall Zn:Pb:Cu proportions, 10:3:1, for the four main mineralized zones. Furthermore, cobalt is absent in the ore minerals, as in Zn–Pb–Cu deposits, but obvious in many Cu–Zn deposits, such as Besshi, in which the pyrite contains ~1,000 ppm Co. Thus, Cofer appears to have Zn–Pb–Cu characteristics in a geological setting of the Cu–Zn group.

TABLE 3. COMPARISON OF TETRAHEDRITE SERIES WITH GRAPHIC INTERGROWTH

Ideal tetrahedrite series	(Cu,	Ag)$_{10}$	(Fe,	Zn)$_2$		(As,	Sb,	Bi)$_4$	S$_{13}$
Cofer tetrahedrite series	Cu$_{9.0}$	Ag$_{0.9}$	Fe$_{1.5}$	Zn$_{0.6}$		As$_{1.6}$	Sb$_{2.4}$	Bi$_{0.2}$	S$_{12.3}$
Graphic intergrowth	Cu$_{3.2}$	Ag$_{0.3}$	Fe$_{7.3}$	Zn$_{0.6}$	Pb$_{0.02}$	As$_{4.0}$	Sb$_{0.02}$	Bi$_{0.1}$	S$_{10.6}$

DISCUSSION

The bulk of the ore minerals (pyrite, sphalerite, chalcopyrite, galena, and others) at Cofer are interpreted to have formed through exhalative-sedimentary processes in a marine volcaniclastic environment, and then to have been subjected to subsequent recrystallization during amphibolite-facies metamorphism. The remainder were formed by exsolution, decomposition, or metasomatism.

In many parts of the ores, pyrite enveloped interstitial minerals during growth and recrystallization. Rarely,

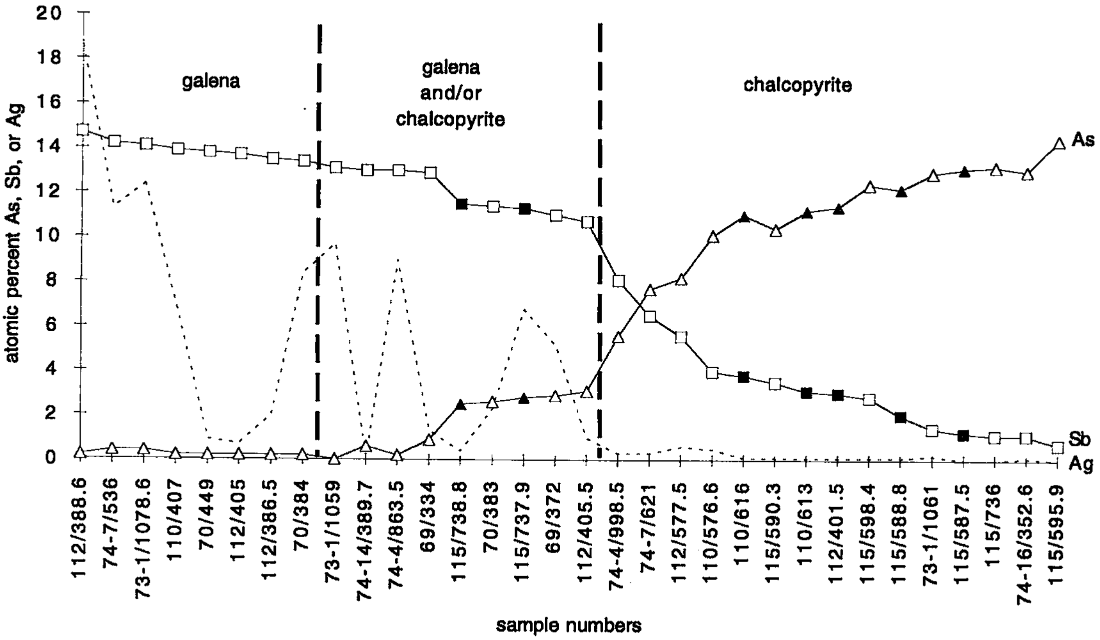

FIG. 10. Galena and chalcopyrite mineral associations with tetrahedrite-series minerals, plotted in order of increasing arsenic and decreasing antimony. Silver content is shown by the dashed line, and samples associated or in contact with arsenopyrite are indicated by solid pairs of symbols.

euhedral inclusions of rutile needles or molybdenite flakes may appear in pyrite; other grains contain large inclusions of galena (≤0.3 mm) that occur in pyrite but not in the matrix. Some samples of ore contain pyrite with perfectly concentric growth-zoning that exhibits tiny inclusions (≤0.005 mm) composed of quartz, rutile, and calcite (Figs. 6a, b). The coincidental zoning of arsenic in pyrite (Fig. 6c) is attributed typically to changes in the composition of the ore fluid (Fleet *et al.* 1989), but may have been caused by "rapid and chaotic changes in the free energy of the pyrite–arsenopyrite system on a very local scale" (Griffin *et al.* 1991). The latter seems more plausible at Cofer, given the relatively narrow field of stability in terms of sulfur activity (see discussion below) and given that realms of stability in ore-forming environments can be on the order of millimeters (Stanton 1976).

Pyrrhotite–chalcopyrite inclusions in pyrite may have been primary phases early in the formation of the Cofer deposit, as observed in modern hydrothermal vent deposits on the sea floor. There, pyrrhotite is observed in plume smoke but not in chimneys, in which the original pyrrhotite has been replaced by pyrite and marcasite or chalcopyrite (Goldfarb *et al.* 1983). Alternatively, pyrrhotite at Cofer may have formed by decomposition of cubanite or intermediate solid-solution upon cooling. The mackinawite, recognized as a low-temperature phase, could not have survived the peak of metamorphism, and thus must have formed during or after the retrograde period. Its distribution is much like that ascribed to exsolution processes by Miyazaki *et al.* (1974) and Ramdohr (1980).

Several copper sulfides occur at Cofer, but only chalcopyrite seems to be primary. Bornite, covellite, digenite, and chalcocite formed by supergene alteration of other sulfides and are restricted to near the surface or to areas of significant flow of groundwater. Marcasite also formed by supergene processes. It is scattered in small amounts throughout the deposit, but any primary marcasite would have been destroyed by metamorphism.

Tetrahedrite, freibergite, and tennantite are widely distributed along with the graphic intergrowth, and likely formed in three ways: (1) deposition syngenetic with the host rock, (2) metasomatism, and (3) exsolution. Tetrahedrite-series minerals found throughout the ore as equant grains probably were deposited with the primary ore minerals, which were syngenetic with the host rock. The graphic intergrowth, which appears to be a product of decomposition of tetrahedrite-series minerals, is more problematical in origin. This texture has been described elsewhere (Ramdohr 1938, Betekhtin 1955, Genkin 1958, Tarantov & Gavrilina 1969, Bespayev *et al.* 1971, Miller & Craig 1983,

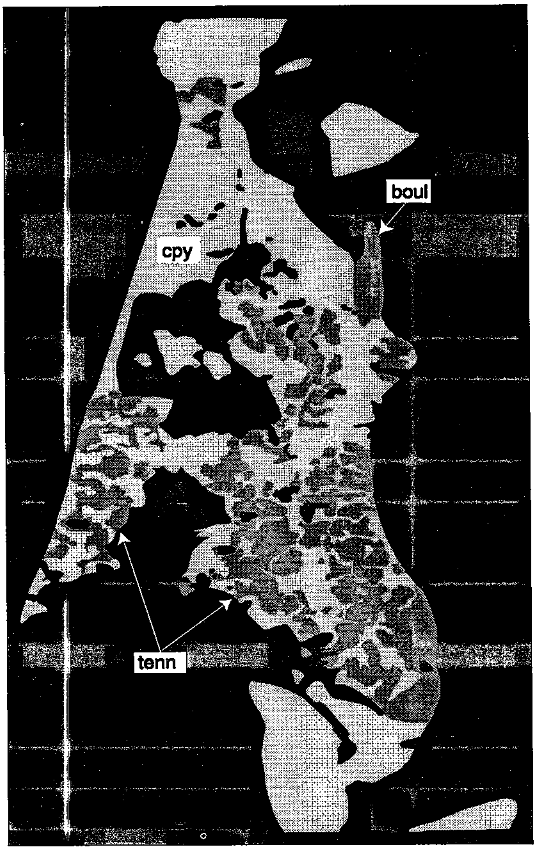

FIG. 11. Intergrowth of tennantite and chalcopyrite. Sample 74–4/887, field of view: 0.27 mm.

Sandecki & Amcoff 1981, Basu *et al.* 1984, and Höller & Gandhi 1995), and much of the speculation on its formation has been summarized by Basu *et al.* (1984). Most of the purported mechanisms involved decomposition of tetrahedrite-series minerals caused by pressure effects, cooling, and interaction with residual solutions. A simple retrograde reaction was proposed (Höller & Gandhi 1995) for the intergrowth at Rampura Agucha, India, where tetrahedrite–freibergite and pyrite decomposed to chalcopyrite ± sphalerite, plus gudmundite or pyrargyrite or both, depending on silver content of the tetrahedrite–freibergite. This reaction is certainly plausible, but a chemical disparity occurs at Rajpura–Dariba (Basu *et al.* 1984) and Cofer, where the parent (Sb-rich) tetrahedrite apparently decomposes to an As-rich intergrowth. A simple decomposition reaction cannot produce a bulk composition of tennantite from tetrahedrite, and furthermore, tennantite should be more refractory than tetrahedrite. Tennantite melts at 665°C (Maske & Skinner 1971), and tetrahedrite melts at 543°C (Tatsuka & Morimoto 1973). Metasomatic replacement was indicated for the texture at Rajpura–Dariba, specifically causing enrichment of Fe, S, and As with depletion of Cu, Zn, Ag, and Sb (Basu *et al.* 1984). A similar reaction involving metasomatic replacement could have occurred at Cofer, but with enrichment of Fe and As, depletion of Cu, Ag, Sb, and S, and no change in Zn. Metasomatic replacement probably is responsible also for the replacement of tennantite by chalcopyrite (Fig. 11), which may have occurred contemporaneously with the formation of the Cu *versus* Zn/Pb zoning of the deposit.

Tetrahedrite and freibergite commonly are in contact with galena and included in it. Exsolution is the likely cause of this texture, as was suggested for Garpenberg Norra (Sandecki & Amcoff 1981). However, if the tetrahedrite–freibergite were present during the metasomatic event that formed the graphic intergrowth, the tetrahedrite–freibergite would have been replaced by arsenopyrite + chalcopyrite + other minerals. Therefore, the exsolution must have occurred after metasomatism and probably during cooling after metamorphism, which is similar to the sequence inferred for Garpenberg Norra (Sandecki & Amcoff 1981).

Native bismuth is a common inclusion in sulfosalts. It may have formed as a syngenetic interstitial phase, trapped subsequently by adjacent crystallizing sulfides, like many of the inclusions in pyrite. Alternatively, exsolution during metamorphism and recrystallization may have produced bismuth, or it may have formed by decomposition or alteration of a sulfosalt phase during formation of the graphic intergrowth.

Classical methods used in estimating conditions of annealing [$f(S_2)$: Toulmin & Barton (1964), T: Kretschmar & Scott (1976), and P: Scott & Barnes (1971)] are of little value at the Cofer deposit, because they require primary pyrrhotite in equilibrium with the analyzed assemblages. However, the existence of arsenopyrite and pyrite, and the absence of native arsenic and pyrrhotite, define a relatively limited field on a log activity of S_2 *versus* 1/T (K) plot. This field can be narrowed using temperatures of equilibration calculated for nearby deposits in the Chopawamsic Formation, if one assumes that the Cofer deposit formed under similar conditions. Fe–Mg distribution in garnet–biotite pairs from the Arminius mine indicates 465°C (Cox 1979), and Zn–Fe distribution in gahnite–biotite pairs from the Julia deposit and Sulphur mine indicates 470°C (Sandhaus & Craig 1986). The combination of mineral assemblages and temperature of equilibration suggests the log of sulfur activity to be in the range of –4.5 to –6.3 atmospheres (Fig. 12).

The distribution of the ore minerals at Cofer indicates that the general direction of the source of mineralization was to the northeast. Cu–Zn zoning at volcanogenic massive sulfide deposits begins with original precipitation of fine-grained black ore (mostly sphalerite, galena, pyrite, and barite). The black ore is subsequently coarsened through continuous interaction

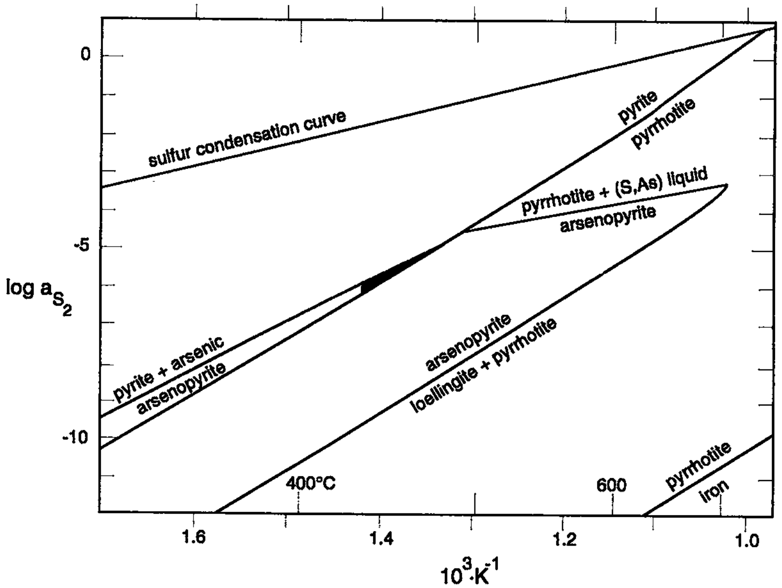

FIG. 12. Log *a*(S2) *versus* 1/T plot illustrating region of thermal maximum for ore minerals of the Cofer deposit (after Barton & Skinner 1979).

with hydrothermal fluids, which leads to replacement of the black ore with yellow ore, and later, pyrite ore (Eldridge *et al.* 1983). Therefore; the volcanic source at Cofer should be closer to the yellow ore and farther from the black ore, which is to the northeast. If this observation is combined with the suggestion of Duke & Hodder (1986) that the massive sulfides were discharged from relatively nearby cross-fractures created by a rapidly spreading rift, then the discharge sites at Cofer should be nearby and to the northeast of the deposit. Conversely, Pavlides *et al.* (1982) indicated that a location for the source of the mineralizing fluids for the base-metal deposits in the Mineral District could have been stockwork-like rocks found near the Julia deposit, to the southwest. Probably the conduit that mineralized Cofer was different from the one that mineralized Julia, in consideration of the 900-meter stratigraphic separation between Cofer and Julia, as well as the zoning of mineralization at Cofer.

CONCLUSIONS

The Cofer deposit contains pyrite, sphalerite, galena, and chalcopyrite, which are typical of volcanogenic massive sulfide deposits. A wide variety of lead – arsenic – antimony – bismuth sulfosalts, native bismuth, and electrum occur also. At least three processes have affected formation of ore minerals at the Cofer deposit: (1) initial deposition from submarine volcanogenic exhalation, (2) interaction with a changing fluid, and (3) metamorphism. During the formation of the Lower Cambrian Chopawamsic Formation, submarine vents emitted bimodal volcanic rocks and the major and minor sulfides and sulfosalts. These were interlayered with clastic sediments. Evolution of the ore fluid caused the crude Zn–Pb *versus* Cu zoning in the deposit and probably formed the graphic intergrowth of arsenopyrite + chalcopyrite at the expense of tetrahedrite–freibergite. Subsequent metamorphism during the Ordovician period and thereafter caused recrystallization of ore minerals and exsolution of many sulfosalts, including tetrahedrite and freibergite associated with galena. Activity of sulfur during re-equilibration at approximately 470°C was in the range of –4.5 to –6.3 atmospheres.

The Cofer deposit resembles both the Zn–Pb–Cu and Cu–Zn deposits of Franklin (1990). The proportion of metals, their zonal distribution at Cofer, and a lack of a stockwork underlying the mineralized bodies recall Zn–Pb–Cu-type deposits, but the composition of host rocks, shape of the orebodies, and lack of a nearby domal eruptive center recall Cu–Zn deposits.

ACKNOWLEDGEMENTS

Thanks are due R.F. Kazda and R.W. Hodder for their technical assistance and consultation on regional geology, Callahan Mining Corporation for technical and financial support, and Piedmont Mineral Associates for permission to work on the Cofer deposit.

We especially appreciate suggestions from R.W. Hodder, B.A. Bouley, R.H. Carpenter, and two other reviewers that greatly improved the manuscript. We are grateful also to Mr. T.N. Solberg for his help with the electron-microprobe analyses.

REFERENCES

ALBEE, A.L. & RAY, L. (1970): Correction factors for electron-probe microanalysis of silicates, oxides, carbonates, phosphates, and sulfates. *Anal. Chem.* **42**, 1408-1414.

BARTON, P.B., JR. & BETHKE, P.M. (1987): Chalcopyrite disease in sphalerite: pathology and epidemiology. *Am. Mineral..* **72**, 451-467.

________ & SKINNER, B.J. (1979): Sulfide mineral stabilities. *In* Geochemistry of Hydrothermal Ore Deposits (2nd edition, H.L. Barnes, ed.). John Wiley & Sons, New York, N.Y. (278-403).

BASU (SANYAL), K., BORTNIKOV, N.S., MISHRA, B., MOOKHERJEE, A., MOZGOVA, N.N. & TSEPIN, A.I. (1984): Significance of transformation textures in fahlores from Rajpura–Dariba polymetallic deposit, Rajasthan, India. *Neues Jahrb. Mineral., Abh.* **149**, 143-161.

BESPAYEV, H.A., PRONIN, A.P. & SLYUSAREV, A.I. (1971): On the stability of sulphosalts in the polymetallic deposits of Rudny Altai. *Izvest. Acad. Sci. Kaz. S.S.R., Geol. Ser.* **1**, 48-56 (in Russ.).

BETEKHTIN, A.G. (1955): Hydrothermal solutions, their nature and the ore formation process. *In* Major Problems in the Study of Magmatic Ore Deposits (A.G. Betekhtin, ed.). *Izd-vo Akademii nauk SSSR,* Moscow, Russia (125-275; in Russ.).

BROWN, C.B. (1937): Outline of the geology and mineral resources of Goochland County, Virginia. *Virginia Geol. Surv. Bull.* **48**.

COX, L.J. (1979): *Mineralogy and Petrogenesis of the Arminius Deposit, Louisa County, Virginia.* M.S. thesis, Virginia Polytech. Inst. State Univ., Blacksburg, Va.

CRAIG, J.R. & VOKES, F.M. (1993): The metamorphism of pyrite and pyritic ores: an overview. *Mineral. Mag.* **57**, 3-18.

CURRIER, L.W. (1935): Zinc and lead region of southwestern Virginia. *Virginia Geol. Surv. Bull.* **43**.

DALLA SALDA, L.H., CINGOLANI, C.A. & VARELA, R. (1992a): The early Paleozoic orogenic belt of the Andes in southwestern South America: result of Laurentia–Gondwana collision? *Geology* **20**, 617-620.

________, DALZIEL, I.W.D., CINGOLANI, C.A. & VARELA, R. (1992b): Did the Taconic Appalachians continue into southern South America? *Geology* **20**, 1059-1062.

DALZIEL, I.W.D. (1997): Neoproterozoic–Paleozoic geography and tectonics: review, hypothesis, environmental speculation. *Geol. Soc. Am., Bull.* **109**, 16-42.

________, DALLA SALDA, L.H. & GAHAGAN, L.M. (1994): Paleozoic Laurentia – Gondwana interaction and the origin of the Appalachian–Andean mountain system. *Geol. Soc. Am., Bull.* **106**, 243-252.

DRAKE, A.A., SINHA, H.K., LAIRD, J. & GUY, R.E. (1989): The Taconic orogen. *In* The Appalachian–Ouachita orogen in the United States (R.D. Hatcher, ed.). The Geological Society of America. Boulder, Colorado (**F-2**, 101-178).

DUKE, N.A. (1983): *A Metallogenic Study of the Central Virginian Gold–Pyrite belt.* Ph.D. thesis, Univ. Manitoba, Winnipeg, Manitoba.

________ & HODDER, R.W. (1986): Stratabound base metals and gold in iron-rich rocks of a late Proterozoic – early Palaeozoic rift setting, central Appalachia, USA. *Trans. Geol. Soc. S. Afr.* **89**, 233-241.

ELDRIDGE, C. S., BARTON, P.B., JR. & OHMOTO, H. (1983): Mineral textures and their bearing on formation of the Kuroko orebodies. *Econ. Geol., Monogr.* **5**, 241-281.

FISHER, G.W. (1970): Introduction [to the Piedmont]. *In* Studies of Appalachian Geology: Central and Southern (G.W. Fisher, F.J. Pettijohn, J.C. Reed, Jr. & K.N. Weaver, eds.). John Wiley & Sons, Inc., New York, N.Y. (295-298).

FLEET, M.E., MACLEAN, P.J. & BARBIER, J. (1989): Oscillatory-zoned As-bearing pyrite from strata-bound and stratiform gold deposits: an indicator of ore fluid evolution. *In* The Geology of Gold Deposits: the Perspective in 1988 (R.R. Keays, W.R.H. Ramsay & D.I. Groves, eds.). *Econ. Geol., Monogr.* **6**, 356-362.

FRANKLIN, J.M. (1990): Volcanic-associated massive sulphide deposits. *In* Gold and Base-Metal Mineralization in the Albitibi Subprovince, Canada (S.E. Ho, F. Robert & D.I. Groves, eds.). *Geology Key Centre and Univ. Extension, Univ. Western Australia, Publ.* **24**, 211-241.

________, LYDON, J.W. & SANGSTER, D.F. (1981): Volcanic associated massive sulphide deposits. Econ. Geol., 75th Anniv. Vol., 485-627.

GAIR, J.E. (1978): Drill core, Mineral district. *U.S. Geol. Surv., Open File Rep.* **78-1068**, 32-52.

GENKIN, A.D. (1958): The phenomena of decomposition of ore minerals. *In* Structure and Texture of Ores (A.G. Betekhtin, A.D. Genkin, A.A. Philomonova & T.N. Shadlun, eds.). State Scientific and Technical Publish. House of Geology Literature, Moscow Russia (248-258) (in Russ.).

GOLDFARB, M.S., CONVERSE, D.R. HOLLAND, H.D. & EDMOND, J.M. (1983): The genesis of hot spring deposits on the East Pacific Rise, 21° N. *Econ. Geol., Monogr.* **5**, 184-197.

GRIFFIN, W.L., ASHLEY, P.M., RYAN, C.G., SOEY, H.S. & SUTER, G.F. (1991): Pyrite geochemistry in the North Arm epithermal Ag–Au deposit, Queensland, Australia: a proton-microprobe study. *Can. Mineral.* **29**, 185-198.

GROSH, W.A. (1949a): Investigation of Valzinco lead–zinc mine, Spotsylvania County, Va. *U.S. Bur. Mines, Rep. Inv.* **4403**.

________ (1949b): Investigation of the Allah Cooper lead–zinc mine, Louisa County, Va. *U.S. Bur. Mines, Rep. Inv.* **4604**.

HICKMAN, R.C. (1947): Pyrites, Mineral, Louisa County, Va. *U.S. Bur. Mines, Rep. Inv.* **4116**.

HODDER, R.W., KAZDA, R.F. & BOJTOS, P. (1977): A base metal massive sulphide deposit within a turbidite succession of the Virginia Piedmont. *Mining Eng.* **29**(1), 83 (abstr.).

HOLDEN, R.J. (1905): The brown ores of the New River – Cripple Creek District, Virginia. *U.S. Geol. Surv., Bull.* **285**, 190-193.

HÖLLER, W. & GANDHI, S.M. (1995): Silver-bearing sulfosalts from the metamorphosed Rampura Agucha Zn–Pb–(Ag) deposit, Rajasthan, India. *Can. Mineral.* **33**, 1047-1057.

HORTON, J.W., JR., DRAKE, A.A., JR. & RANKIN, D.W. (1989): Tectonostratigraphic terranes and their Paleozoic boundaries in the central and southern Appalachians. *In* Terranes in the Circum-Atlantic Paleozoic Orogens (R.D. Dallmeyer, ed.). *Geol. Soc. Am., Spec. Publ.* **230**, 213-245.

HUTCHINSON, R.W. (1973): Volcanogenic sulfide deposits and their metallogenic significance. *Econ. Geol.* **68**, 1223-1246.

HUTCHISON, M.N. & SCOTT, S.D. (1979): Application of the sphalerite geobarometer to Swedish Caledonide and U.S. Appalachian metamorphosed massive sulfide ores. *In* Symposium on Caledonian–Appalachian stratabound sulphide deposits (Trondheim, Norway), 14-15 (abstr.).

JEFFERSON, T. (1794): Notes on the State of Virginia (2nd ed.). Philadelphia, Pennsylvania.

KASE, K. (1977): Sulfide minerals and their assemblages of the Besshi deposit. *Mining Geol. (Japan)* **27**, 355-365.

KRETSCHMAR, U. & SCOTT, S.D. (1976): Phase relations involving arsenopyrite in the system Fe–As–S and their application. *Can. Mineral.* **14**, 364-386.

LARGE, R.R. (1977): Chemical evolution and zonation of massive sulfide deposits in volcanic terrains. *Econ. Geol.* **72**, 549-572.

LONSDALE, J.T. (1927): Geology of the gold–pyrite Belt of the northeastern Piedmont Virginia. *Virginia Geol. Surv. Bull.* **30**.

LUTTRELL, G.W. (1966): Base- and precious-metal and related ore deposits of Virginia. *Virginia Div. Mineral Resources, Rep.* **7**.

MASKE, S. & SKINNER, B.J. (1971): Studies of the sulfosalts of copper. I. Phases and phase relations in the system Cu–As–S. *Econ. Geol.* **66**, 901-918.

MILLER, J.W. & CRAIG, J.R. (1983): Tetrahedrite–tennantite series compositional variations in the Cofer deposit, Mineral district, Virginia. *Am. Mineral.* **68**, 227-234.

MIYAZAKI, K., MUKAIYAMA, H. & IZAWA, E. (1974): Thermal metamorphism of the bedded cupriferous iron sulfide deposit at the Besshi mine, Ehime Prefecture, Japan. *Mining Geol. (Japan)* **24**, 1-12.

MOOKHERJEE, A. (1976): Ores and metamorphism: temporal and genetic relationships. *In* Handbook of Strata-bound and Stratiform Ore Deposits **4** (K.H. Wolf, ed.). Elsevier, Amsterdam, The Netherlands (203-260).

MORTON, R.L. & FRANKLIN, J.M. (1987): Two-fold classification of Archean volcanic-associated massive sulfide deposits. *Econ. Geol.* **82**, 1057-1063.

PAVLIDES, L. (1981): The Central Virginia volcanic–plutonic belt: an island arc of Cambrian (?) age. *U.S. Geol. Surv., Prof. Pap.* **1231-A**, 1-34.

________, GAIR, J.E. & CRANFORD, S.L. (1982): Central Virginia volcanic–plutonic belt as a host for massive sulfide deposits. *Econ. Geol.* **77**, 233-272.

POOLE, J.L. (1973): Iron sulfide mines in Virginia. *Virginia Minerals* **19**, 29-33.

RAMDOHR, P. (1938): Antimonreiche Paragenesen von Jakobsbaken bei Sulitelma. *Norsk Geol. Tidsskr.* **18**, 275-289.

________ (1980): *The Ore Minerals and their Intergrowths* (second ed.). Pergamon Press, Oxford, U.K.

RICHARDS, S.M. (1966): Mineragraphy of fault-zone sulphides, Broken Hill, N.S.W. *C.S.I.R.O. Mineragraphic Inv. Tech. Pap.* **5**.

SALMON, B.C., CLARK, B.R. & KELLY, W.C. (1974): Sulfide deformation studies. II. Experimental deformation of galena to 2,000 bars and 400 Deg. C. *Econ. Geol.* **69**, 1-16.

SANDECKI, J. & AMCOFF, Ö. (1981): On the occurrence of silver-rich tetrahedrite at Garpenberg Norra, central Sweden. *Neues Jahrb. Mineral., Abh.* **141**, 324-340.

SANDHAUS, D.J. & CRAIG, J.R. (1986): Gahnite in the metamorphosed stratiform massive sulfide deposits of the Mineral district, Virginia, U.S.A. *Tschermaks Mineral. Petrogr. Mitt.* **35**, 77-98.

SANGSTER, D.F. & SCOTT, S.D. (1976): Precambrian strata-bound, massive Cu–Zn–Pb sulfide ores of North America. *In* Handbook of Strata-bound and Stratiform Ore Deposits **6** (K.H. Wolf, ed.). Elsevier, Amsterdam, The Netherlands (129-222).

SATO, T. (1974): Distribution and geological setting of the Kuroko deposits. *Soc. Mining Geol. Japan, Spec. Issue* **6**, 1-10.

SAUER, R.T. (1983): *A Metamorphosed Stratiform Alteration Zone as Footwall to Massive Sulfide, Mineral District, Virginia.* M.S. thesis, Univ. Western Ontario, London, Ontario.

SAWKINS, F.J. (1976): Massive sulphide deposits in relation to geotectonics. *Geol. Assoc. Can., Spec. Pap.* **14**, 221-240.

SCOTT, S.D. & BARNES, H.L. (1971): Sphalerite geothermometry and geobarometry. *Econ Geol.* **66**, 653-669.

________, BOTH, R.A. & KISSIN, S.A. (1977): Sulfide petrology of the Broken Hill region, New South Wales. *Econ Geol.* **72**, 1410-1425.

SEAL, R.R., II, ESSENE, E.J. & KELLY, W.C. (1990): Tetrahedrite and tennantite: evaluation of thermodynamic data and phase equilibria. *Can. Mineral.* **28**, 725-738.

SHANMUGAM, G. & LASH, G.G. (1982): Analogous tectonic evolution of the Ordovician foredeeps, southern and central Appalachians. *Geology* **10**, 562-566.

SHIMAZAKI, Y. (1974): Ore minerals of the Kuroko-type deposits. *Soc. Mining Geol. Japan, Spec. Issue* **6**, 311-322.

SOLOMON, M. (1976): "Volcanic" massive sulphide deposits and their host rocks – a review and an explanation. *In* Handbook of Strata-bound and Stratiform Ore Deposits **6** (K.H. Wolf, ed.). Elsevier, Amsterdam, The Netherlands (21-50).

SOUTHWICK, D.L., REED, J.C., JR. & MIXON, R.B. (1971): The Chopawamsic Formation – a new stratigraphic unit in the Piedmont of northeastern Virginia. *U.S. Geol. Surv., Bull.* **1324-D**, 1-10.

STANTON, R.L. (1976): Petrochemical studies of the ore environment at Broken Hill, New South Wales. 2. Regional metamorphism of banded iron formations and their immediate associates. *Inst. Mining Metall. Trans.* **85**, B118-B131.

SWEET, P.C. (1971): Gold mines and prospects in Virginia. *Virginia Minerals* **17**, 25-33.

TARANTOV, A.S. & GAVRILINA, K.S. (1969): On a decomposition of fahlore with the formation of arsenopyrite and chalcopyrite. *In* Methods of Investigation of Substance Composition and their Application **II** (B.S. Khristoforov, ed.). Nauka, Siberian Branch, Novosibirsk, Russia (in Russ.; 104-111).

TATSUKA, K. & MORIMOTO, N. (1973): Composition variation and polymorphism of tetrahedrite in the Cu–Sb–S system below 400°C. *Am. Mineral.* **58**, 425-434.

TOULMIN, P., III & BARTON, P.B., JR. (1964): A thermodynamic study of pyrite and pyrrhotite. *Geochim. Cosmochim. Acta* **28**, 641-671.

VOKES, F.M. (1969): A review of the metamorphism of sulphide deposits. *Earth Sci. Rev.* **5**, 99-143.

WATSON, T.L. (1907): *Mineral Resources of Virginia.* J.P. Bell Company, Lynchburg, Virginia.

WIGGINS, L.B. & CRAIG, J.R. (1980): Reconnaissance of the Cu–Fe–Zn–S system: sphalerite phase relationships. *Econ. Geol.* **75**, 742-751.

WILLIAMS, H. & HATCHER, R.D., JR. (1982): Suspect terranes and accretionary history of the Appalachian orogen. *Geology* **10**, 530-536.

YUI, S. (1970): Heterogeneity with a single grain of minerals of the tennantite–tetrahedrite series. *Soc. Mining Geol. Japan, Spec. Issue* **2**, 22-29.

Received February 25, 1997, revised manuscript accepted October 13, 1997.

APPENDIX I.

SAMPLING AND ANALYTICAL PROCEDURES

The examination and description of the Cofer deposit were based on 286 polished sections, taken from 13 diamond drill-holes (186 sections) and the 160- and 340-foot (49- and 104-m) drifts. These sections were selected from 474 available samples as being representative of the deposit.

Mineral chemistry was determined primarily with an Applied Research Laboratories Scanning Electron Microprobe Quantometer equipped with a Kevex 500 X-ray energy-dispersion spectrometer, located at the Department of Geological Sciences, Virginia Polytechnic Institute and State University. The electron microprobe was operated at 15 kV, a beam current of 10 nA, and a counting time of 20 seconds. The Bence–Albee method was used for data reduction (Albee & Ray 1970). The standards selected were checked against each other, and against other synthetic simple sulfides.